Supplemental Information for

Cell motility and migration as determinants of stem cell efficacy

Lusine Danielyan[1,2*], Matthias Schwab[1,2,3,4], Georg Siegel[5], Bianca Brawek[6], Olga Garaschuk[6], Nithi Asavapanumas[6], Marine Buadze[1], Ali Lourhmati[1], Hans-Peter Wendel[7], Meltem Avci-Adali[7], Marcel A. Krueger[8], Carsten Calaminus[8], Ulrike Naumann[9], Stefan Winter[3], Elke Schaeffeler[3], Annett Spogis[1], Sandra Beer-Hammer[10], Jonas J. Neher[11,12], Gabriele Spohn[13], Anja Kretschmer[13], Eva-Maria Krämer-Albers[14], Kerstin Barth[14], Hong Jun Lee[15,16], Seung U. Kim[17], William H. Frey II[18], Claus D. Claussen[19], Dirk M. Hermann[20],Thorsten R. Doeppner[20,21], Erhard Seifried[13], Christoph H. Gleiter[1], Hinnak Northoff[5] & Richard Schäfer[5,13]

[1]Department of Clinical Pharmacology, University Hospital Tübingen, Tübingen, Germany

[2] Neuroscience Laboratory and Departments of Biochemistry and Clinical Pharmacology, Yerevan State Medical University, Yerevan, Armenia

[3]Dr. Margarete Fischer-Bosch Institute of Clinical Pharmacology, Stuttgart, Germany and University of Tübingen, Tübingen, Germany

[4]Department of Pharmacy and Biochemistry, University of Tübingen, Tübingen, Germany

[5]Institute of Clinical and Experimental Transfusion Medicine, University Hospital Tübingen, Tübingen, Germany

[6]Institute of Physiology, Department of Neurophysiology, University of Tübingen, Tübingen, Germany

[7]Department of Thoracic, Cardiac and Vascular Surgery, University Hospital Tübingen, Tübingen, Germany

[8]Werner Siemens Imaging Center, Department of Preclinical Imaging and Radiopharmacy, University Hospital Tübingen, Tübingen, Germany

[9]Hertie Institute for Clinical Brain Research and Center Neurology, Department of Vascular Neurology, Tübingen Neuro-Campus (TNC), University of Tübingen, Tübingen, Germany

[10]Department of Pharmacology, Experimental Therapy and Toxicology, Institute of Experimental and Clinical Pharmacology and Pharmacogenomic, and ICePhA, University Hospital Tübingen, Tübingen, Germany

[11]Department of Cellular Neurology, Hertie Institute for Clinical Brain Research, University of Tübingen, Tübingen, Germany

[12]German Center for Neurodegenerative Diseases (DZNE), Tübingen, Tübingen, Germany

[13]Institute for Transfusion Medicine and Immunohematology, German Red Cross Blood Donor Service Baden-Württemberg-Hessen gGmbH, Goethe-University Hospital, Frankfurt am Main, Germany

[14]Institute for Developmental Biology and Neurobiology, Johannes Gutenberg University Mainz, Mainz, Germany

[15]College of Medicine and Medical Research Institute, Chungbuk National University, Cheongju, Chungbuk, Republic of Korea;,

[16] Research Institute eBiogen Inc., Seoul, Republic of Korea

[17]Division of Neurology, Department of Medicine, UBC Hospital, University of British Columbia, Vancouver, BC, Canada

[18]HealthPartners Center for Memory and Aging, HealthPartners Neurosciences, St. Paul, MN, U.S.A.

[19]Department of Radiology, University Hospital Tübingen, Tübingen, Germany

[20]Department of Neurology, University of Duisburg-Essen, Essen, Germany

[21]Department of Neurology, University Medical Center Göttingen, Göttingen, Germany

This file includes Supplementary Figures 1-6

Supplementary Figure 1

a

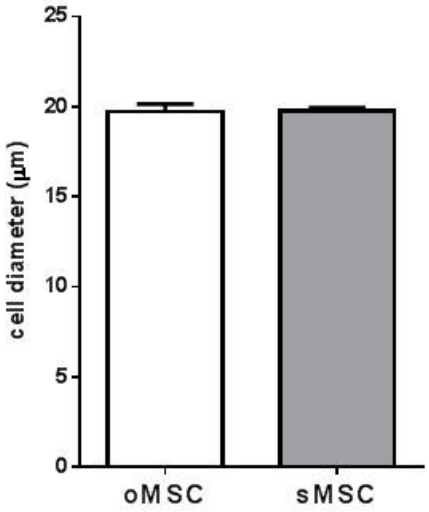

b

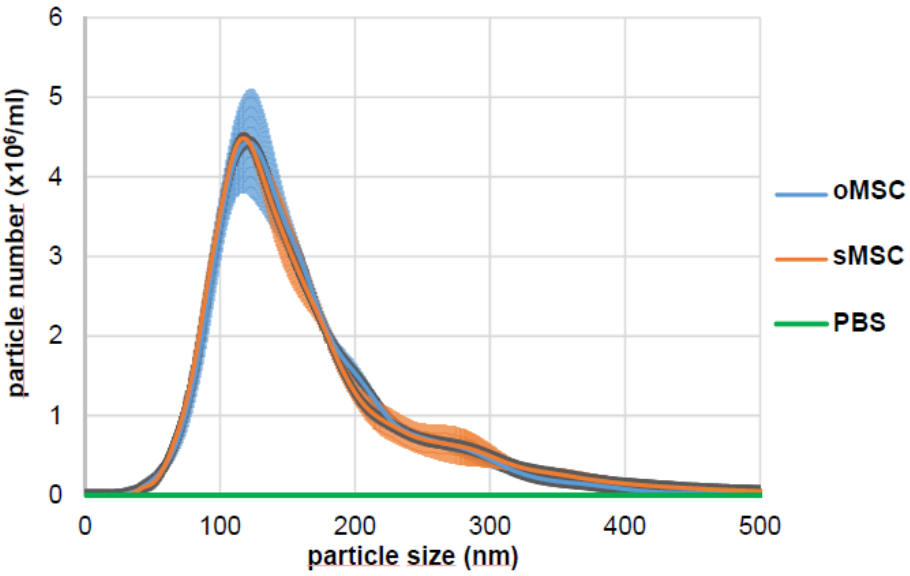

	oMSC	sMSC
Mean size (nm)	159 +/-2.8	164 +/-7.8
Total number (10^8 particles/ml)	5.06 +/-0.6	4.5 +/-0.5

c

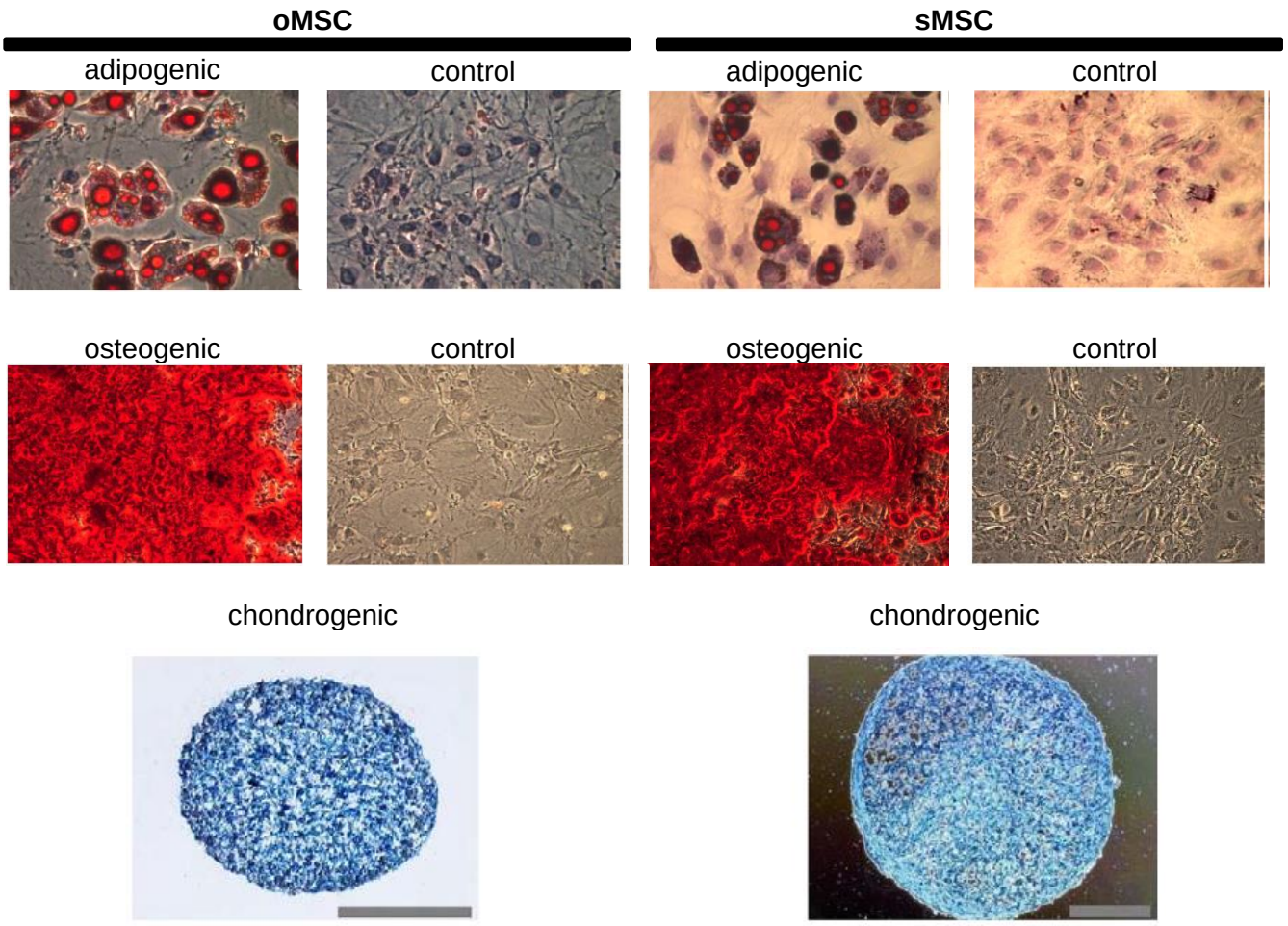
oMSC
sMSC
adipogenic
control
adipogenic
control
osteogenic
control
osteogenic
control
chondrogenic
chondrogenic

d

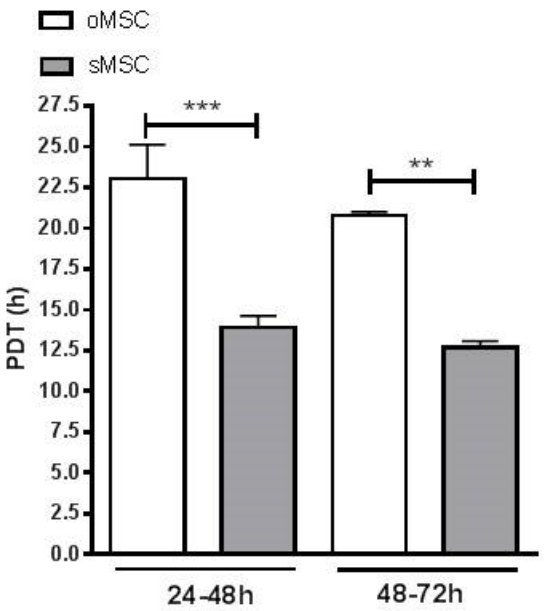
oMSC
sMSC
PDT (h)
27.5
25.0
22.5
20.0
17.5
15.0
12.5
10.0
7.5
5.0
2.5
0.0
***
**
24-48h
48-72h

e

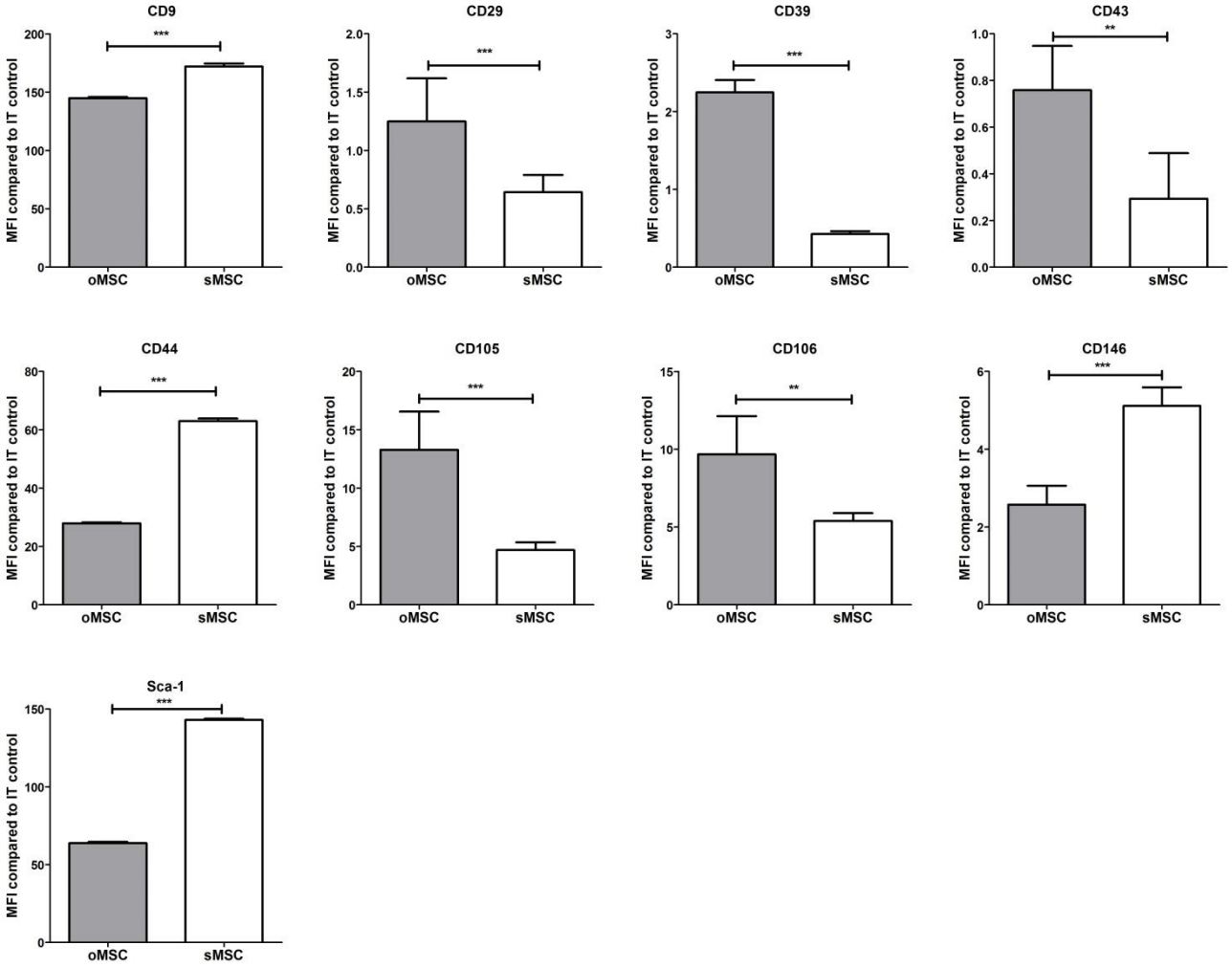

Supplementary Figure 1. Characterization of murine oMSC and sMSC.

a, morphology assessed by cell diameter. Mean cell diameter did not differ between oMSC (19.73 µm ±1.22 µm SD) and sMSC (19.75 µm ±0.57 µm SD), n=9 per group; two-tailed t-test. Error bars: SEM. **b**, nanoparticle tracking analysis of small extracellular vesicles (small-EVs) derived from oMSC and sMSC (n=3). EVs were isolated by differential centrifugation. Final 100.000 x g pellets were re-suspended in PBS and size-distribution of EVs was determined by laser-based particle tracking. EVs secreted from oMSC and sMSC do not differ in size and amount. Error bars: SEM. Mean particle size and the total number of particles (area under the curve) collected from each sample type are denoted in the table below the graph. **c**, in vitro differentiation capacity. No differences of in vitro differentiation potential could be detected between oMSC and sMSC. Lipid vacuoles of adipogenically differentiated MSC are stained in red with Oil-Red-O, calcium deposits of osteogenic differentiated MSC are stained in red with

Alizarin Red S, and chondrogenic differentiation of MSC pellets are stained in bluish-green by Alcian blue. Original magnifications: 200x (adipogenic, control), 100x (osteogenic, control), 4x (chondrogenic [scale bars: 500 µm]). **d**, in vitro growth kinetics. Population doubling time (PDT) was determined between 24-48 h and 48-72 h after seeding of cells onto the cell culture dish n=3; One-way ANOVA with Bonferroni's multiple comparisons test (**p <0.01, oMSC vs. sMSC at 48-72 h; ***p<0.001, oMSC vs. sMSC at 24-48 h). Error bars: SEM. **e**, flow cytometry analyses of mean fluorescence intensity (MFI). sMSC featured higher expression of CD9 (Tspan29), CD44 (H-CAM), CD146 (MCAM) and Sca-1 on sMSC, whereas CD29 (Integrin β1), CD39 (ENTPD1), CD43 (Sialophorin), CD105 (Endoglin), CD106 (VCAM-1) were higher expressed on oMSC, n=3; two-tailed t-test (*p<0.05; **p <0.01; ***p<0.001). Error bars: SD.

Supplementary Figure 2

a

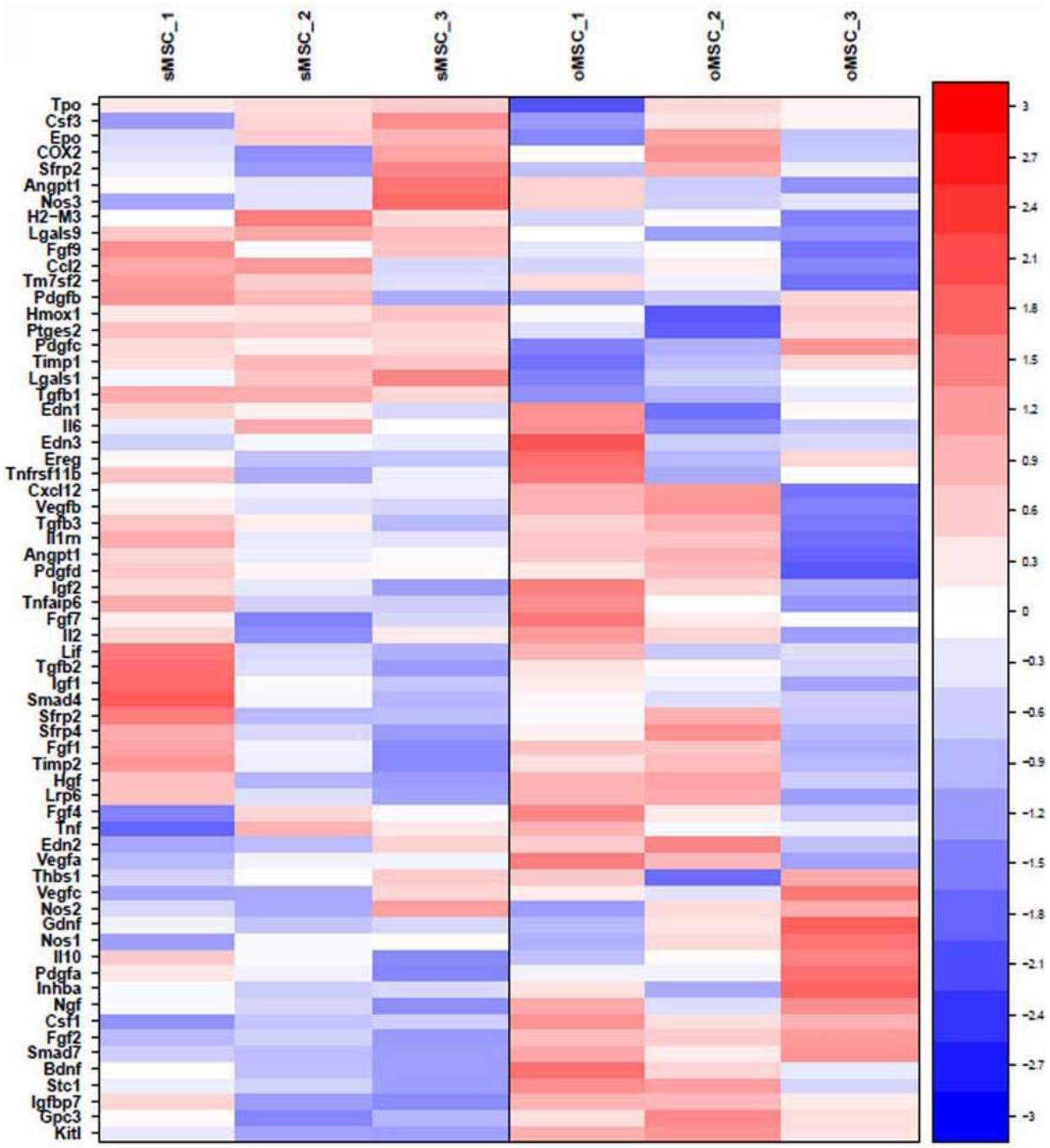

b

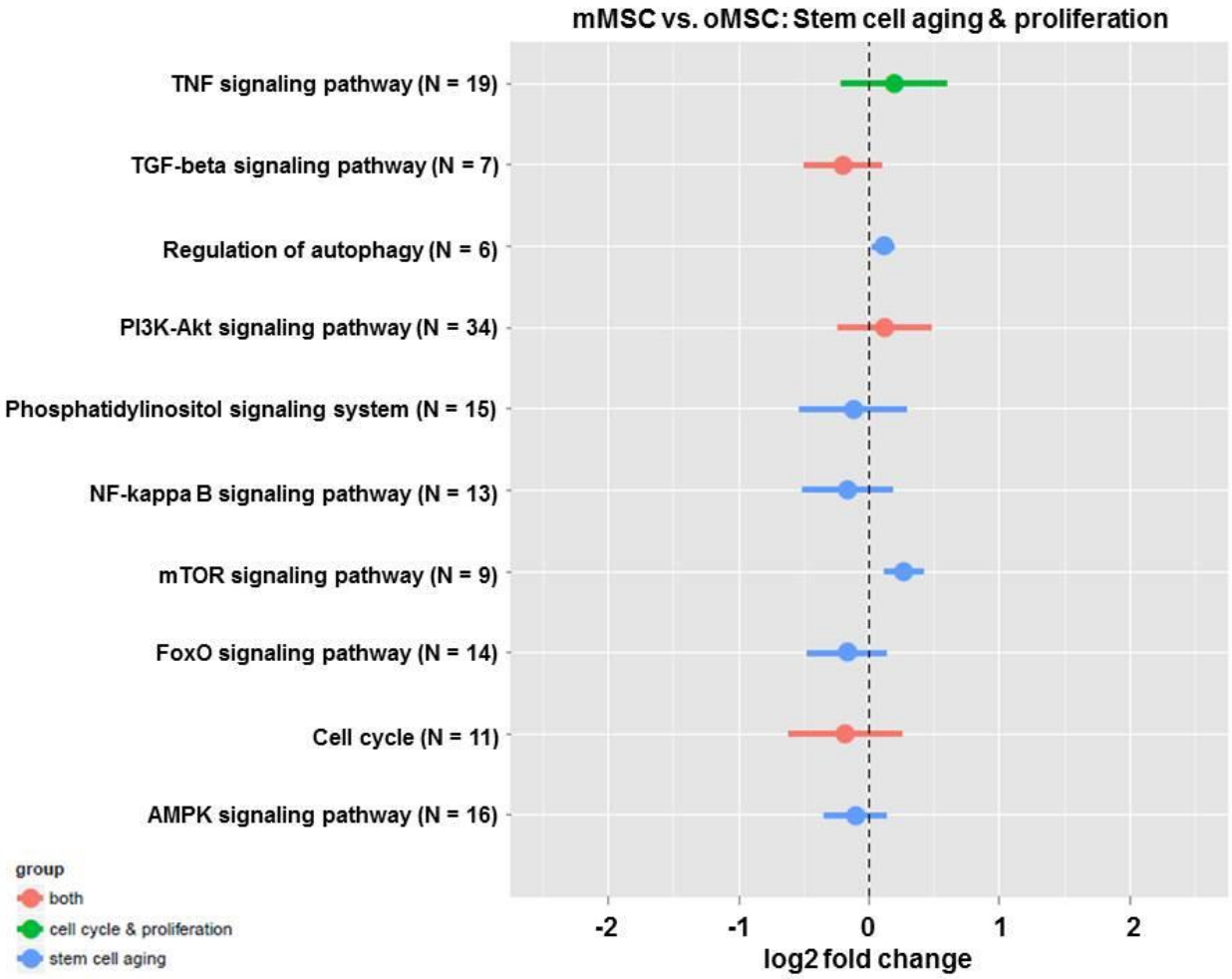

Supplementary Figure 2. Microarray analysis of murine oMSC and sMSC.

a, heatmap of microarray data displaying genes related to trophic factors, thereby highlighting - in contrast to genes involved in cell migration and/or adhesion - considerable heterogeneity between passages. The heatmap shows row-wise z-scores of normalized log2 signal intensities in murine oMSC and sMSC; n=3 arrays per group (3 different passages). Genes are ordered according to complete-linkage hierarchical clustering based on Pearson correlation coefficients, which were calculated across all six arrays. Z-scores were color-coded as indicated by the colorbar on the right. Of all the genes displayed, only *Smad7* differed significantly and relevantly between sMSC and oMSC (p=0.048, FC=0.45) **b**, median effect sizes ± MAD (median absolute deviation) between murine oMSC and sMSC for KEGG mouse pathways related to stem cell aging and cell cycle & proliferation. For each pathway, the median and MAD were calculated

based on all corresponding genes, which show a significant difference between oMSC and sMSC ($p<0.05$); the number of those genes is given in brackets. For each gene, the effect size was defined as median across the log2 fold change (sMSC/oMSC) in each of the three passages.

Supplementary Figure 3

a

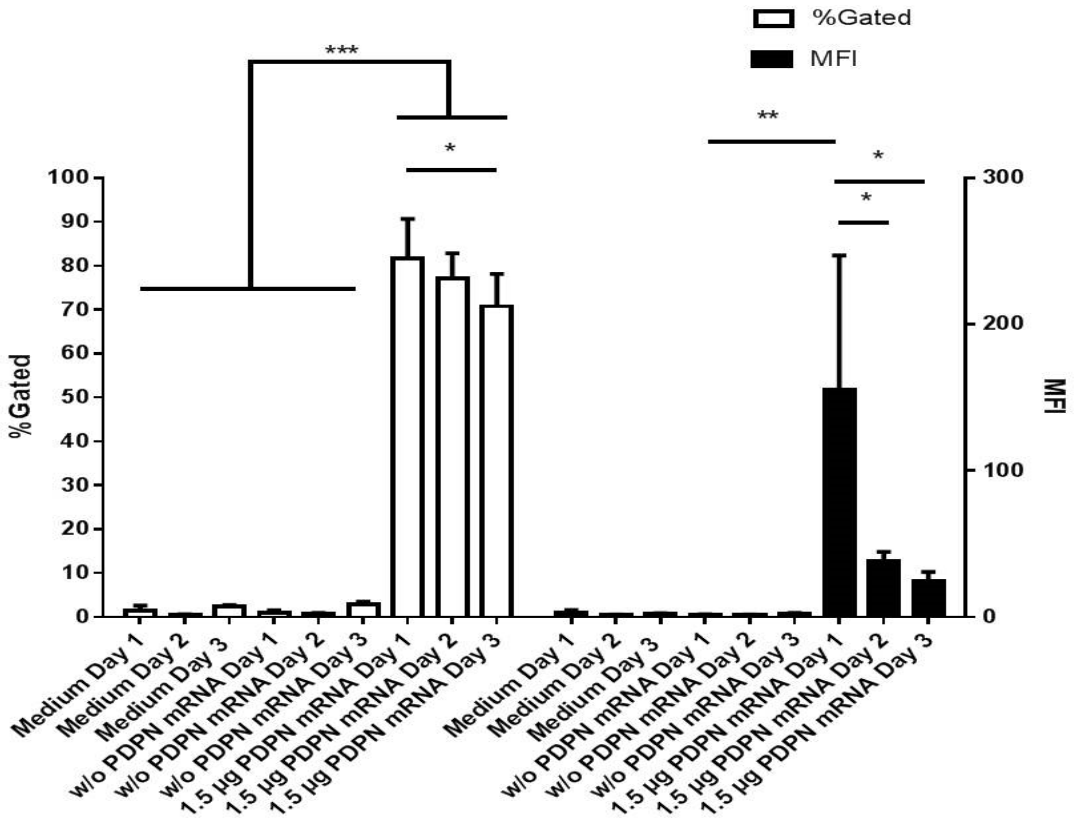

b

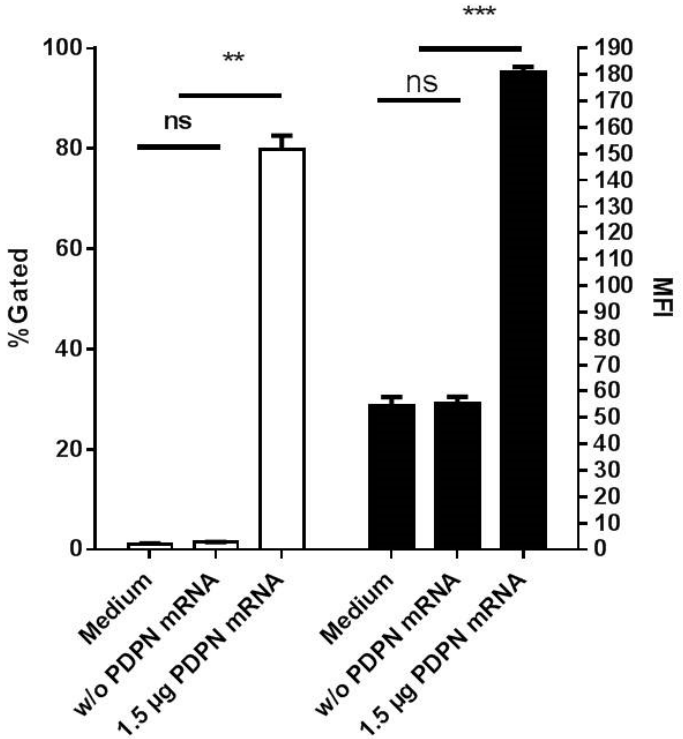

Supplementary Figure 3. Evaluation of podoplanin engineering of oMSC and oHB1.F3 NSC.

a, flow cytometry analysis of PDPN protein on days 1-3 after transfection of murine oMSC (P64, P72) with either transfection vehicle, transfection medium, or 1.5 µg PDPN mRNA, n=3; One-way ANOVA with Bonferroni's multiple comparisons test (*p<0.05; **p <0.01; ***p <0.001). Error bars: SEM. **b**, flow cytometry analysis of PDPN protein 72 h after transfection of human HB1.F3 NSC with either transfection vehicle, transfection medium, or 1.5 µg PDPN mRNA, n=3; One-way ANOVA with Bonferroni's multiple comparisons test (**p <0.01; ***p <0.001). Error bars: SEM.

Supplementary Figure 4

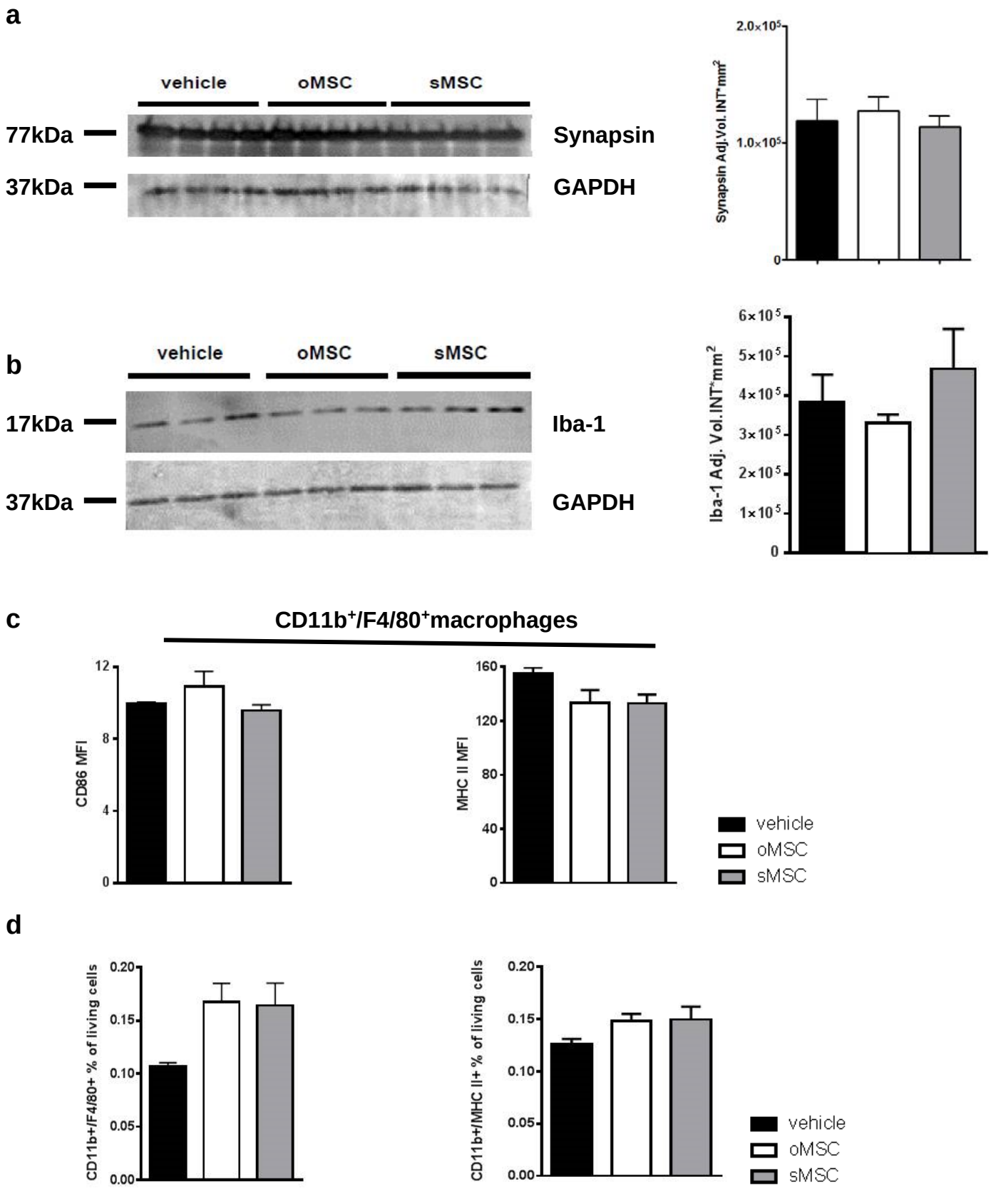

e

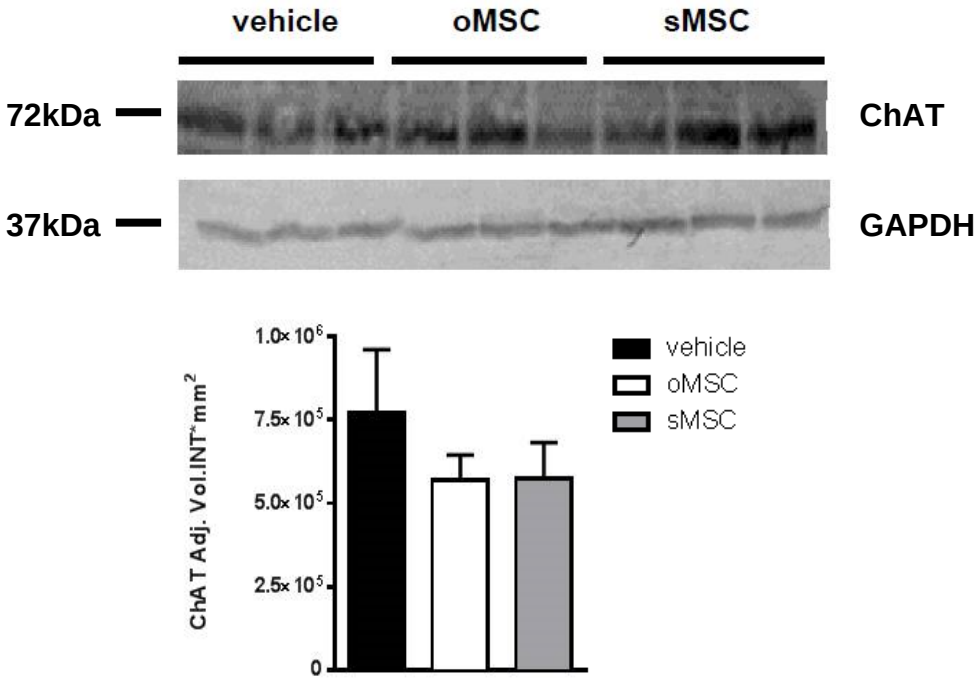
vehicle
oMSC
sMSC
72kDa
ChAT
37kDa
GAPDH
ChAT Adj. Vol.INT*mm2
1.0× 10^6
7.5× 10^5
5.0× 10^5
2.5× 10^5
0
vehicle
oMSC
sMSC

f

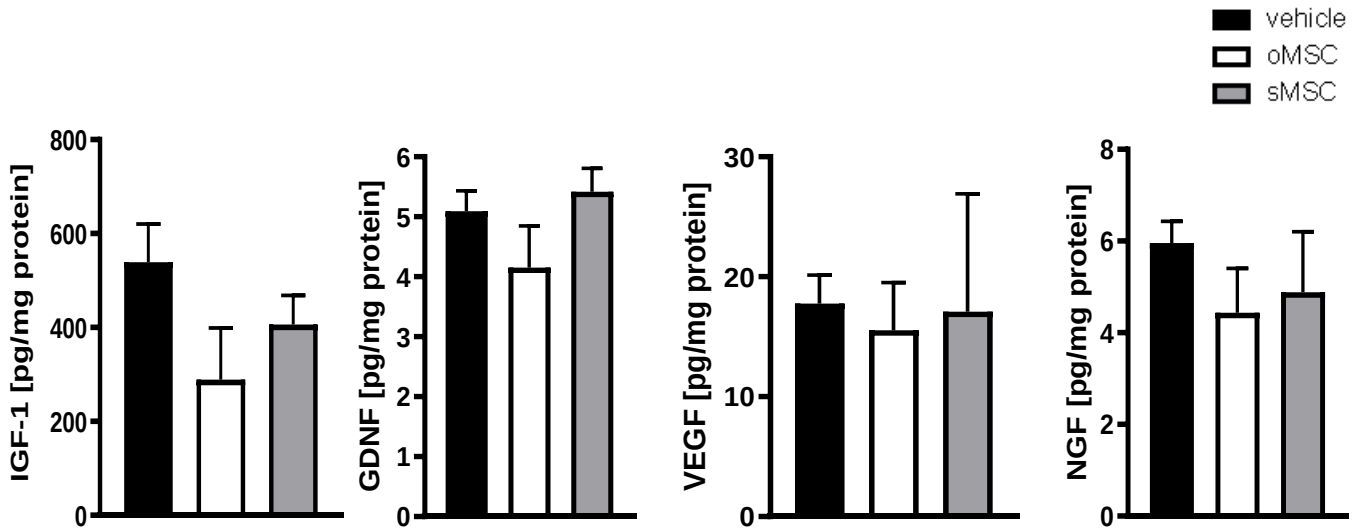
vehicle
oMSC
sMSC
IGF-1 [pg/mg protein]
800
600
400
200
0
GDNF [pg/mg protein]
6
5
4
3
2
1
0
VEGF [pg/mg protein]
30
20
10
0
NGF [pg/mg protein]
8
6
4
2
0

g

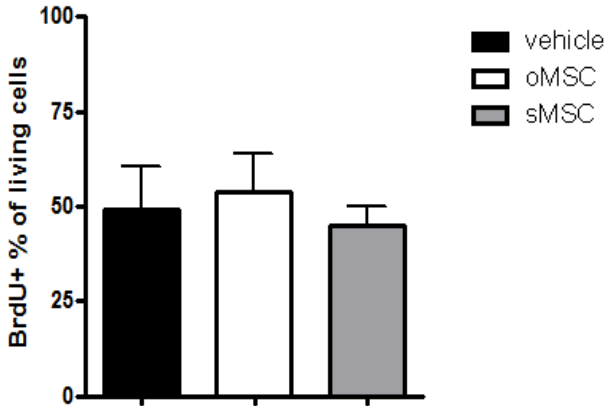
BrdU+ % of living cells
100
75
50
25
0
vehicle
oMSC
sMSC

Supplementary Figure 4. In vivo concentrations of trophic factors and immune cells after murine oMSC or sMSC transplantation in the murine 3xTg-AD model.

a, Western blot with densitometric analysis of synapsin in brain homogenates of 13-month old 3xtg-AD mice after INA of oMSC and sMSC. One-way ANOVA with Bonferroni's multiple comparisons test, n=4. Error bars: SEM. **b**, Western blot with densitometric analysis of Ionized Calcium-binding Adapter Molecule (Iba)-1 in brain homogenates of 13-months old 3xtg-AD mice after INA of oMSC and sMSC, n=3; One-way ANOVA with Bonferroni's multiple comparisons test. Error bars: SEM. **c**, flow cytometry analyses of CD86 and MHC II (both markers of M1 polarization of macrophages) in CD11b+ /F4/80+ macrophages from brain cells suspensions of 13-months old 3xtg-AD mice after INA of sMSC and oMSC, n=3; One-way ANOVA with Bonferroni's multiple comparisons test. Error bars: SEM. **d**, INA of oMSC and sMSC did not change the number of M1 macrophages reflected by total percentage of CD11b/MHC II+ cells and by mean fluorescence intensity (MFI) of CD86 and MHC II in CD11b+/F4/80+ macrophages, n=3; One-way ANOVA with Bonferroni's multiple comparisons test. Error bars: SEM. **e**, Western blot with densitometric analysis of Choline Acetyltransferase (ChAT) in brain homogenates of 13-months old 3xtg-AD mice after INA of oMSC and sMSC, n=3; One-way ANOVA with Bonferroni's multiple comparisons test. Error bars: SEM. Densitometric analyses of ChAT, synapsin and Iba-1 are shown as adjusted volume intensity x mm^2 normalized to the GAPDH. **f**, quantification of insulin-like growth factor (IGF)-1, glial cell line-derived neurotrophic factor (GDNF), vascular endothelial growth factor (VEGF) and nerve growth factor (NGF) by ELISA in brain homogenates of 13-months old 3xtg-AD mice after INA of oMSC and sMSC, n=3-6; One-way ANOVA with Bonferroni's multiple comparisons test. Error bars: SEM. **g**, flow cytometry analysis of BrdU+ cells from brain suspensions of 13-month old 3xtg-AD mice after INA of sMSC and oMSC. BrdU was injected intraperitoneally (0.03 mg/kg BW) and added to drinking water (1mg/mL) 3 days prior to sacrifice, n=3; One-way ANOVA with Bonferroni's multiple comparisons test. Error bars: SEM.

Supplementary Figure 5

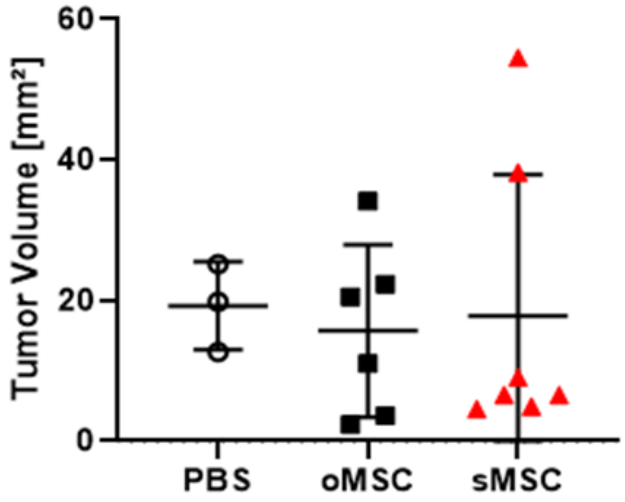

Supplementary Figure 5. Tumour size of oMSC and sMSC treated C57/BL6 mice after GL-261 implantation.

Tumours assessed by MRI as shown in the main Figure 8 were analysed by manual tumour volume determination. Data and means are shown for oMSC (n=6), sMSC (n=7) and vehicle (PBS, n=3) groups 21 days post GL261-luc injection. One-way ANOVA with Bonferroni's multiple comparisons test. Error bars: SEM.

Supplementary Figure 6

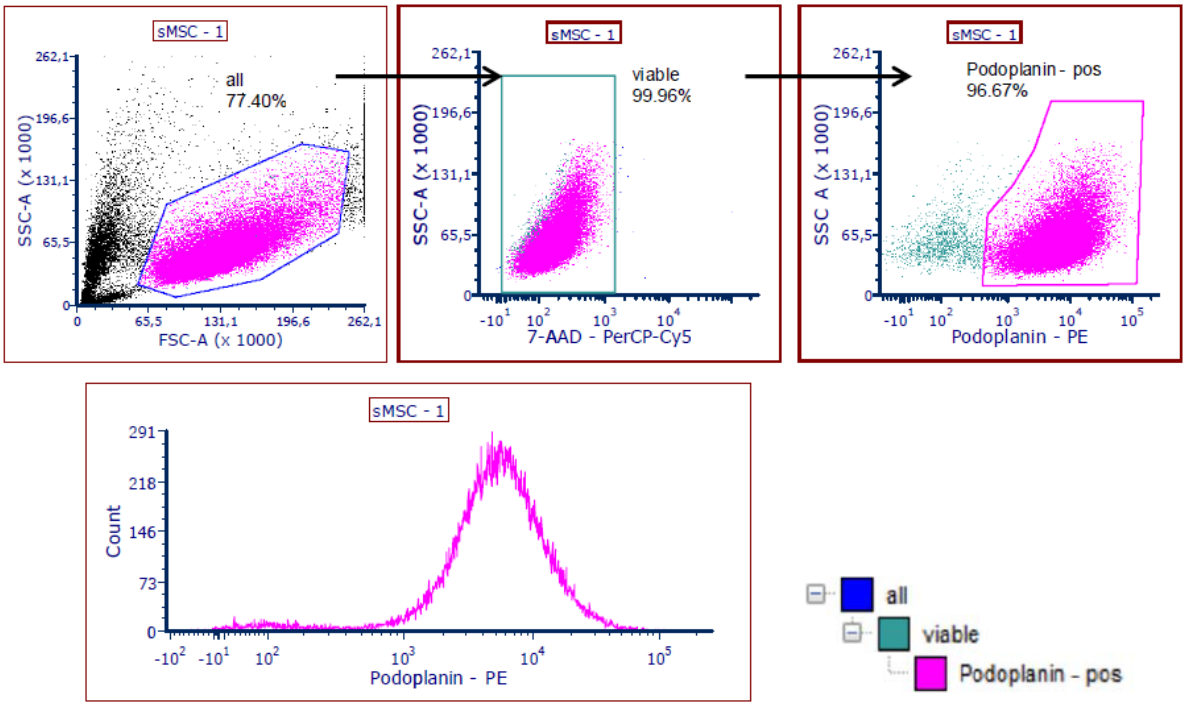

Supplementary Figure 6. Flow cytometry gating strategy.

Exemplary flow cytometry plots and histogram show the gating strategy of podoplanin expression analysis on sMSC. Non-viable cells were identified and excluded from further analysis by 7-AAD staining.

Uncropped gels

Fig.3a PDPN

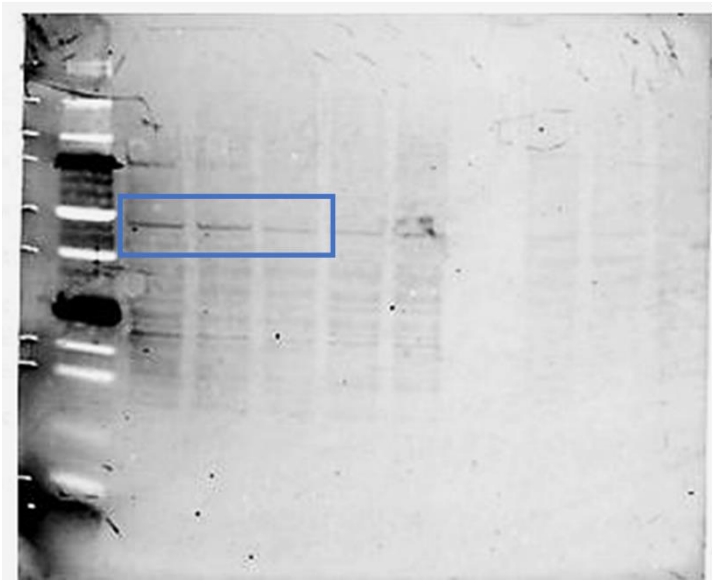

Fig.3a GAPDH

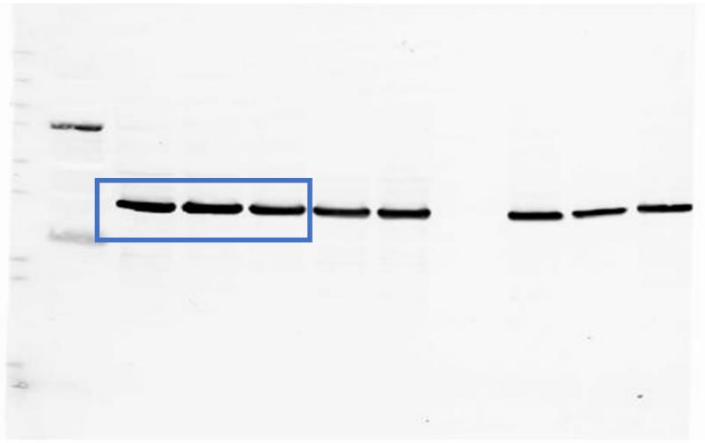

Fig.6c Synaptophysin

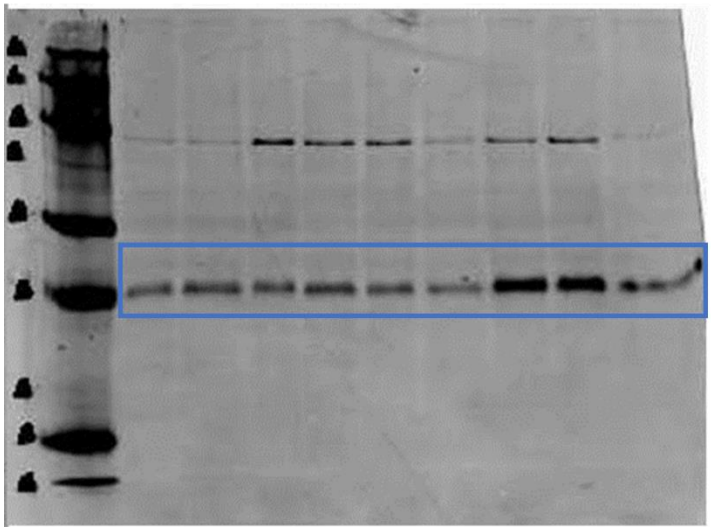

Fig.6c GAPDH

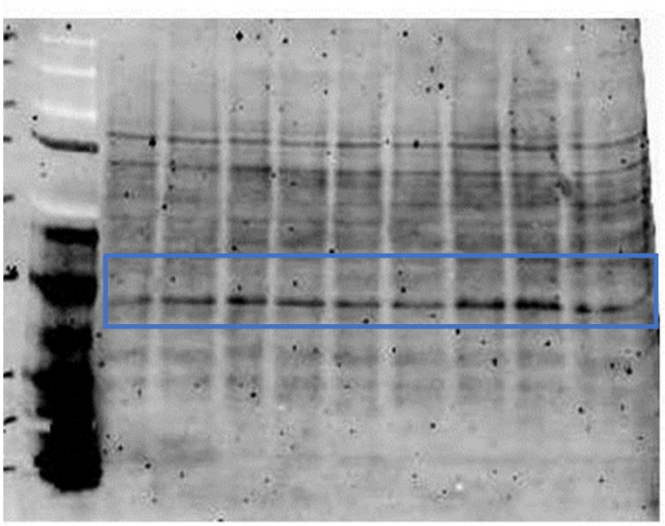

Synapsin Suppl Fig.4a

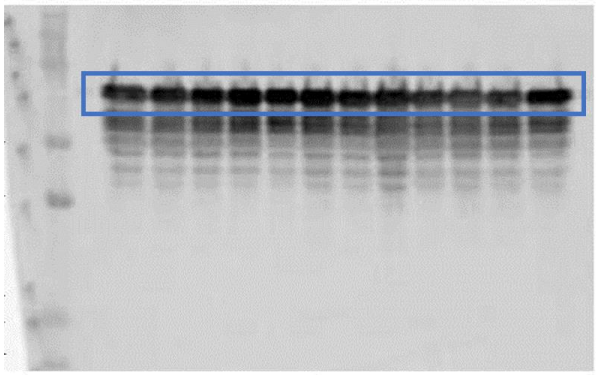

GAPDH Suppl Fig.4a

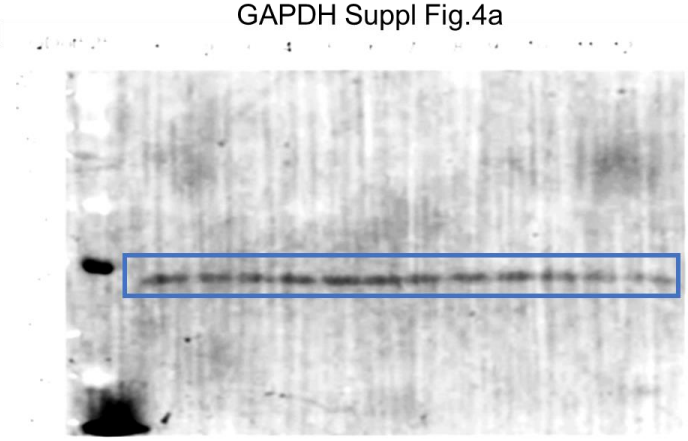

Iba-1 Suppl Fig.4b

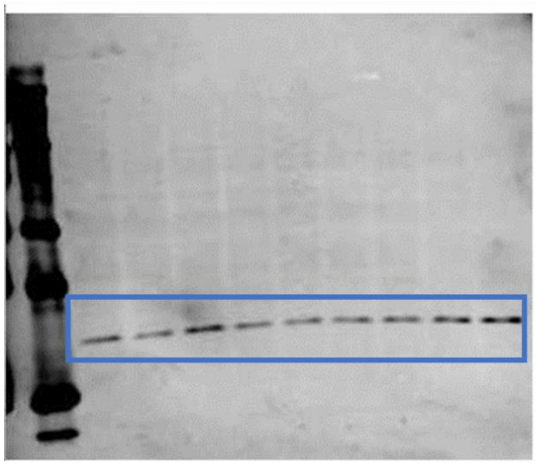

GAPDH Suppl Fig.4b

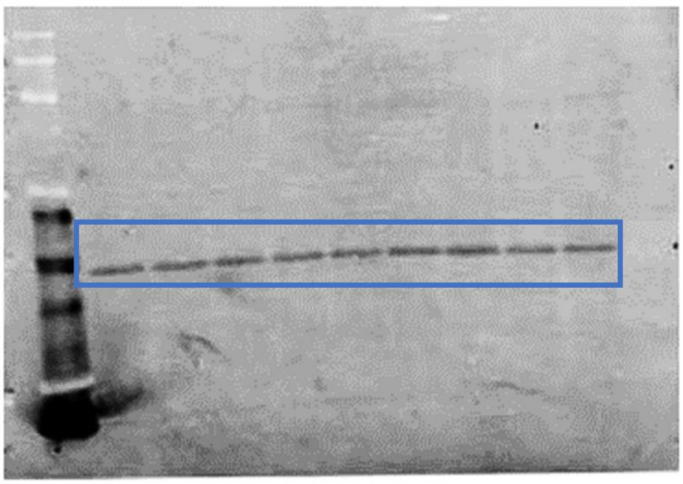

ChAT Suppl Fig.4e

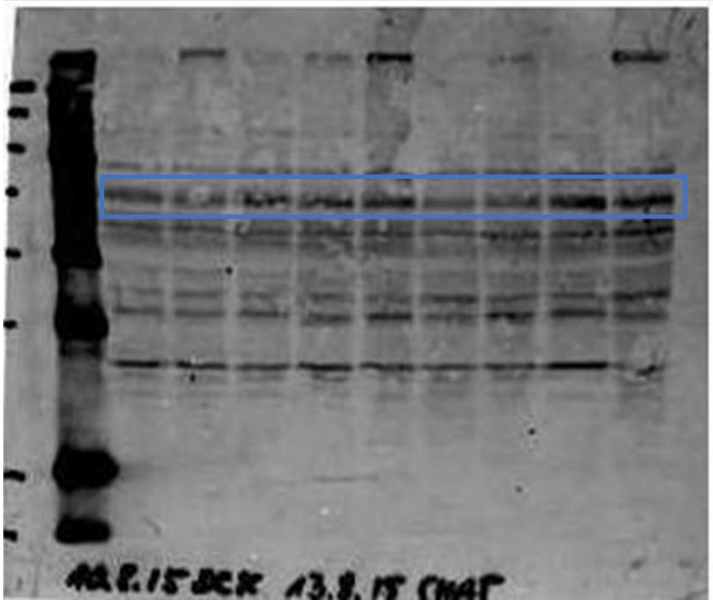

GAPDH Suppl Fig.4e